

Synthesis and magnetic properties of a quantum magnet PbCuTeO_5

B. Koteswararao,¹ S. P. Chilakalapudi,¹ Aga Shahee,² P. V. Srinivasarao,³ S. Srinath,¹ A. V. Mahajan²

¹*School of Physics, University of Hyderabad, Central University PO, Hyderabad 500046, India.*

²*Department of Physics, Indian Institute of Technology Bombay, Mumbai 400076, India.*

³*Department of Physics, Acharya Nagarjuna University, Nagarjuna Nagar 522 510, India.*

Abstract

We report the structural and magnetic properties of a quantum magnet PbCuTeO_5 . The triclinic structure of PbCuTeO_5 comprises of alternating layers (ab -planes), in which one layer is composed of $S = 1/2$ dimer chains and another layer is composed of $S = 1/2$ trimer chains formed by corner-shared CuO_4 units. Magnetic susceptibility $\chi(T)$ data show a Curie-Weiss behavior with an antiferromagnetic Curie-Weiss temperature θ_{CW} of -165 K. At low temperature, both the heat capacity $C_p(T)$ and $\chi(T)$ show an anomaly at $T_c \approx 6$ K with a weak ferromagnetic (WFM) moment suggesting the appearance of long-range order. The magnetization vs. field $M(H)$ data at 2 K also provide evidence for WFM behavior. Magnetic frustration with a frustration parameter $f = \theta_{\text{CW}}/T_c$ of about 27 is observed. Magnetic specific heat data suggest the presence of a large entropy in the paramagnetic region, well above T_c , suggesting the presence of short-range spin correlations. The observed results might originate from the frustrated network of $S = 1/2$ distorted checkerboard lattice formed due to the coupling of the spin chains *via* TeO_6 octahedral units in the ab -plane.

Keywords: PbCuTeO_5 , Geometrical frustration, $S = 1/2$ checkerboard lattice, 2D Pyrochlore lattice.

I. INTRODUCTION

Geometrical frustration can forbid the formation of magnetic long-range order (LRO) even at $T = 0$ K and hence lead to exotic spin ground states such as quantum spin-liquids, according to the initial proposal by P. W. Anderson [1]. The experimental realization of new spin-liquid materials is currently one of the central topics in condensed matter physics. The spin-liquid behavior can be realized in two-dimensional (2D) geometrically frustrated magnetic systems (GFMS) including triangular (edge-shared), Kagome (corner-shared), and checkerboard lattice models [2-4]. In the recent past, Herberthsmithite $\text{ZnCu}_3(\text{OH})_6\text{Cl}_2$, a celebrated Heisenberg antiferromagnet pertaining to the $S = 1/2$, 2D Kagome model, has been the focus of attention [5-10]. In this material, the Cu^{2+} ions ($S = 1/2$) lie on the vertices of a perfect corner-shared triangular lattice, *i.e.*, the Kagome lattice. Magnetic susceptibility data analysis yielded the antiferromagnetic (AFM) Curie-Weiss temperature (θ_{CW}) of about -300 K and the exchange coupling of about $J/k_B \approx -180$ K. No signature of magnetic LRO was found down to 50 mK, claiming that it is a potential candidate for spin-liquid. On the other hand, the organic salt $\text{K}(\text{BEDT-TTF})_2\text{Cu}_2(\text{CN})_3$ was shown to exhibit a gapless spin-liquid state firmly establishing its candidature to the class of 2D edge-shared triangular lattice [11, 12]. While the study of the spin-liquid state in the triangular and Kagome model materials has been extensively advancing,

no materials have yet been reported in the context of checkerboard and/or 2D pyrochlore lattice model which has been predicted theoretically as good candidates for realizing the spin-liquid, valence bond crystal, *etc.* [13-17].

In this paper, we introduce a new quantum spin system PbCuTeO_5 . According to its Cu-O-Cu exchange paths, this compound appears to have spin chains lying in its crystallographic *ab*-plane. However, magnetic data do not exhibit any characteristic feature of spin chain magnetism. Magnetic susceptibility data rather follow a Curie-Weiss behavior with antiferromagnetic Curie-Weiss temperature (θ_{CW}) of about -165 K. At low- T , the system undergoes a transition at $T_c = 6$ K. Specific heat data also show the evidence of large magnetic entropy above T_c . The observed results suggest that frustrated magnetism in the titled system could be originated from a 2D checkerboard lattice (which is one of the model system for highly frustrated magnetic lattice) with anisotropic couplings in the *ab*-plane, which forms due to the coupling between spin chains *via* TeO_6 units in the *ab*-plane.

II. EXPERIMENTAL DETAILS

The polycrystalline PbCuTeO_5 sample was prepared by the conventional solid-state reaction method. The molar mixtures of PbO , CuO , and Te with a ratio of 1:1:1.05 were ground together, pressed into pellets. The additional 5% of Te was added to compensate for the loss due to evaporation during synthesis. We have then fired the sample in air successively at temperatures of 500°C , 600°C , and 720°C . Each firing was done for 12 hrs with an intermediate grinding. Finally, the firing was carried out at 720°C for 24 hrs to get the final phase of the compound. The powder x-ray diffraction measurements were done at room temperature using a Rigaku diffractometer equipped with the monochromator for $\text{Cu-}K_{\alpha 1}$ radiation. The magnetic measurements were performed in the temperature (T) range of 2 to 300 K and in the magnetic field (H) using a SQUID-VSM from Quantum Design. Specific heat measurements were performed by 2τ relaxation method using a Physical Property Measurement System (PPMS) from Quantum Design.

III. RESULTS AND DISCUSSION

A) X-ray diffraction and structural features

To check for the formation of single phase of PbCuTeO_5 sample, the measured powder XRD data was refined with FullProf Suite program [18] using the initial parameters given by Pavlina Choleva [19]. As shown in Figure 1, the refinement of XRD indicates a good fit with the χ^2 value of 6.95. The lattice parameters of this triclinic unit cell are obtained to be $a = 6.431(4)$ Å, $b = 11.317(7)$ Å, $c = 12.31(9)$ Å, $\alpha = 107.9^\circ$, $\beta = 90.9^\circ$, and $\gamma = 90.4^\circ$, which are in agreement with those of previously reported values [19]. The obtained atomic positions are mentioned in the Table 1.

The PbCuTeO_5 compound has triclinic unit cell with the space group $P-1$ (No. 2). As shown in Figure 2, the structure is built by TeO_6 octahedra, CuO_4 distorted squares, and Pb atoms. The Cu atoms lie only in the ab -planes which are in fact well separated from each other by an inter-planar distance of 6.15 Å, thereby forming 2D planes (as shown in Figure 3). The structure has two kind of layers; one at $z = 0$ and the other at $z = 0.5$. The $z = 0$ layer is built by dimer chains, while the $z = 0.5$ layer is built by trimer chains, as shown in Figure 3. The bond angles and bond lengths between Cu-Cu atoms are mentioned in Table II. According to the super-exchange (SE) pathways between Cu atoms *via* O atoms, the bond angles are in the range of 110° to 120° degrees, which likely favors antiferromagnetic bonds according to the Goodenough rules [20]. With the consideration of magnetic super-super-exchange (SSE) bonds between Cu atoms *via* O–Te–O, it is to be suggested that these layers are forming like a distorted checkerboard lattice. As it can be seen from the Figure 3 that there are two types of checkerboard lattices formed with dimer and trimer chains, respectively.

B) Magnetic susceptibility $\chi(T)$ and specific heat at zero-field

Magnetic susceptibility $\chi(T)$ as a function of temperature in the range from 2 K to 300 K is shown in Figure 4. The Inverse magnetic susceptibility $\chi^{-1}(T)$ data show a linear behavior at high- T above 70 K and then the data steeply fall at low- T . Hence, we fitted the data with the below expression in the T -range from 70 K to 300 K.

$$\chi = \chi_0 + \frac{C}{T - \theta_{CW}}$$

The temperature independent susceptibility χ_0 was found to be about $-1 \times 10^{-4} \text{ cm}^3/\text{mol}$, which is a sum of core diamagnetic susceptibility and Van-Vleck susceptibility. The core diamagnetic susceptibility has been calculated to be $-6.3 \times 10^{-5} \text{ cm}^3/\text{mol}$ [21]. The Van-Vleck susceptibility was therefore inferred to be $3.7 \times 10^{-5} \text{ cm}^3/\text{mol}$, which is in agreement with many cuprate systems. The obtained Curie-Weiss constant is $0.51 \text{ cm}^3 \text{ K}/\text{mol}$, which gives an effective magnetic moment of about $2.02 \mu_B$, similar to other Cu-based magnetic materials [22, 23]. The Curie-Weiss temperature (θ_{CW}) is found to be -165 K, indicating the presence of strong AFM correlations in the sample. However, no signature of one dimensional magnetism such as broad maximum in the magnetic susceptibility has been noticed. To further understand the nature of magnetic ground state of this system, we have plotted the χT versus T as shown in Figure 4(b). In this plot, the value of χT at 300 K is $0.32 \text{ cm}^3 \text{ K}/\text{mol}$, which is smaller than the value expected for free $S = 1/2$ value $0.3751 \text{ cm}^3 \text{ K}/\text{mol}$. This can be attributed to the presence of AFM correlations. This claim is further strengthened from the observation of decreasing χT value with decreasing T . At low- T , an anomaly is observed at 6 K ($= T_c$),

indicating the formation of magnetic long-range order due to the presence of weak inter-layer (3D) couplings.

The specific heat (C_p) measurement was carried out in zero-field in the T -range from 2 K to 200 K. $C_p(T)$ has two contributions; lattice and magnetic. To understand the magnetic behavior from the specific heat, we have subtracted the lattice contribution using Debye expression mentioned below.

$$C_p = 9rNk_B \sum_{i=1,2} C_i \left(\frac{T}{\theta_D^i} \right)^3 \int_0^{x_D^i} \frac{x^4 e^x}{(e^x - 1)^2} dx$$

Here r is the number of atoms per formula unit, θ_D is a Debye temperature. The fitting yields $C_1 \approx (0.36 \pm 0.05)$, $\theta_{D1} \approx (180 \pm 5)$ K, $C_2 \approx (0.58 \pm 0.05)$, and $\theta_{D2} \approx (650 \pm 10)$ K. The fitted curve was subtracted from the measured specific heat data. As an outcome, the obtained magnetic contribution is plotted in the inset of Figure 5. Similar to $\chi(T)$ data, a sharp anomaly is observed at 6 K. The entropy change ΔS_m was calculated by integrating the magnetic specific heat divided by T (C_m/T) with respect to T . The value of ΔS_m is reached to the maximum value $R \ln 2$ at 50 K. The value of ΔS_m at the transition is found to be 0.4 J/mol K, which is only 7 % of total entropy. The observation of remaining large entropy in the paramagnetic region (above T_c) suggesting the presence of strong short-range spin correlations. This feature has already been seen in several frustrated spin systems [24, 25].

C) Magnetic data and specific heat in magnetic fields

In order to understand the low- T anomaly, we have performed $\chi(T)$ measurements at different magnetic fields. Below 6 K, $\chi(T)$ data at low fields exhibit the splitting between the data measured under the zero-field-cooled (ZFC) and field-cooled (FC) conditions, as shown in inset of Figure 6(a). With increasing H , the splitting reduces. The anomaly disappears by the magnetic field of 1 T. The similar behavior is also observed in the C_p data (see Figure 6(b)) under magnetic fields. The magnetic anomaly smears out by the field of 1 T. To further confirm the weak-ferromagnetic nature, we measure the $M(H)$ data at different temperatures. At 2 K, the $M(H)$ plot shows magnetic hysteresis (see inset of Figure 6(b)). The coercive field of 0.05 T and the remanance magnetization of $0.003 \mu_B/\text{mol}$ are observed.

The structure suggests that it has linear chains with Cu-O-Cu bond angles of about 110° to 120° . The super-exchange (SE) couplings are approximately expected to be in the range 130 K – 150 K for this bond angle [26, 27] and the obtained θ_{CW} is -160 K for this compound. In this picture, one-dimensional magnetism features such as broad maximum is expected at about 100 K in the $\chi(T)$ and

70 K in $C_m(T)$ data [28]. However, we have not seen such features in the magnetic data. Instead, the features of frustrated magnetism is seen with a large frustration parameter $f = \theta_{CW}/T_c \approx 27$ K. The frustrated magnetism could be due to the formation of geometrical network of checkerboard lattice (distorted) by the coupling of chains in the ab -plane *via* super-super-exchange (SSE) couplings through O-Te-O atoms. Such SSE interactions were observed to be dominant in many compounds $\text{SrCuTe}_2\text{O}_6$ [25], $\text{Na}_2\text{Cu}_2\text{TeO}_6$ [29], $\text{Cu}_2\text{A}_2\text{O}_7$ ($A = \text{V, P, and As}$), *etc* [30-34]. Since the magnetic couplings in the checkerboard layer are highly anisotropic, we might not see the physics of spin-liquid and valance bond solid (VBS) phases, as predicted theoretically [13-17], in this compound.

IV. CONCLUSION

We have successfully prepared the polycrystalline sample of a new quantum magnet PbCuTeO_5 . The structure suggests that it has two layers (ab -planes) of $S = 1/2$ distorted checkerboard lattice, which were formed by the coupling of spin chains. Magnetic susceptibility data exhibit a magnetic anomaly at 6 K despite the presence of large antiferromagnetic Curie-Weiss temperature of about -165 K. Magnetic specific heat data also showed the presence of large magnetic entropy above T_c , confirming the existence of short-range spin correlations owing to frustrated magnetic network of the anisotropic checkerboard lattice. Our preliminary magnetic analysis suggests the presence of strong magnetic frustration in this material. The presence of anisotropic and inter-layer couplings might be the reason to observe the magnetic-LRO, instead of the theoretically predicted disordered state for the ideal $S = 1/2$ checkerboard or 2D pyrochlore lattice. Further, the NMR and μSR local probe measurements will be helpful to understand the spin dynamics of this quantum magnet.

Acknowledgments: B.K. thanks DST INSPIRE faculty award-2014 scheme.

Electronic address: koti.iitb@gmail.com

References

- [1] Anderson P W 1987 *Science* **235** 1196.
- [2] Misguich G and Lhuillier C 2005 *Frustrated Spin Systems*, World Scientific.
- [3] Lacroix C, Mendels P and Mila F 2011 *Introduction to Frustrated Magnetism*.
- [4] Balents L 2010 *Nature (London)* **464** 199.
- [5] Shores M P, Nytko E A, Bartlett B M and Nocera D G 2005 *J. Am. Chem. Soc.* **127** 13462.

- [6] Helton J S, Matan K, Shores M P, Nytko E A, Bartlett B M, Yoshida Y, Takano Y, Suslov A, Qiu Y, Chung J-H, Nocera D G and Lee Y S 2007 *Phys. Rev. Lett.* **98** 107204.
- [7] Lee S H, Kikuchi H, Qiu Y, Lake B, Huang Q, Habicht K and Kiefer K 2007 *Nature Mater.*, **6** 853.
- [8] Olariu A, Mendels P, Bert F, Duc F, Trombe J, De Vries M and Harrison A 2008 *Phys. Rev. Lett.* **100** 087202.
- [9] Imai T, Nytko E A, Bartlett B M, Shores M P and Nocera D G 2008 *Phys. Rev. Lett.* **100** 077203.
- [10] Fu M, Imai T, Han T-H and Lee Y S 2015 *Science* **350** 655.
- [11] Yamashita S, Nakazawa Y, Oguni M, Oshima Y, Nojiri H, Shimizu Y, Miyagawaand K and Kanoda K 2008 *Nature Phys.* **4** 459.
- [12] Yamashita M, Nakata N, Kasahara Y, Sasaki T, Yoneyama N, Kobayashi N, Fujimoto S, Shibauchi T and Yuji Matsuda 2009 *Nature Phys.* **5** 44.
- [13] Moessner R and Chalker J T 1998 *Phys. Rev. B* **58** 12049.
- [14] Lieb E H and Schupp P, 1999 *Phys. Rev. Lett.* **83** 5362.
- [15] Palmer S E and Chalker J T 2001 *Phys. Rev. B* **64** 94412.
- [16] Starykh O A, Furusaki A and Balents L 2005 *Phys. Rev. B* **72** 094416.
- [17] Nussinov Z, Batista C D, Normand B and Trug-man S A 2007 *Phys. Rev. B* **75** 094411.
- [18] Rodríguez-Carvajal J 1993 *Physica B* **192** 55.
- [19] Pavlina Choleva, *PhD thesis*, 2004.
- [20] Goodenough J B 1955 *Phys. Rev.* **100** 564.
- [21] Selwood P W 1956 *Magnetochemistry* 2nd edn (New York: Wiley-Interscience) chapter 2 p 78
- [22] Koteswararao B, Panda S K, Kumar R, Kyongjun Yoo, Mahajan A V, Dasguptha I, Chen B H, Kee Hoon Kim and Chou F C 2015 *J. Phys: Condens. Matter* **27** 426001.
- [23] Koteswararao B, Kumar R, Khuntia P, Sayantika Bhowal, Panda S K, Rahman M R, Mahajan A V, Dasgupta I, Baenitz M, Kee Hoon Kim and Chou F C 2014 *Phys. Rev. B* **90** 035141.

- [24] Alexander L K, Büttgen N, Nath R, Mahajan A V and Loidl A 2007 *Phys. Rev. B* **76** 064429.
- [25] Koteswararao B, Kumar R, Chakraborty J, Jeon B -G, Mahajan A V, Dasgupta I, Kim K H and Chou F C 2013 *J. Phys.: Condens. Matter* **25** 336003.
- [26] Tsirlin A A, Rousochatzakis I, Kasinathan D, Janson O, Nath R, Weickert F, Geibel C, Lauchli A M and Rosner H 2010 *Phys. Rev. B* **82** 144426.
- [27] Shimizu T, Matsumoto T, Goto A, Yoshimura K and Kosuge K 2003 *Physica* **B329-333** 765; Volkova L M, Polyshchuk S A (2005) *Journal of Superconductivity* **18** 583.
- [28] Johnston D C *et al.* 2000 *Phys. Rev. B* **61** 9558.
- [29] Schmitt M, Janson O, Golbs S, Schmidt M, Schnelle W, Richter J and Rosner H 2014 *Phys. Rev. B* **89** 174403.
- [30] Tsirlin A A, Janson O and Rosner H 2010 *Phys. Rev. B* **82** 144416.
- [31] Arango Y C, Vavilova E, Abdel-Hafiez M, Janson O, Tsirlin A A, Rosner H, Drechsler S -L, Weil M, Nénert G, Klingeler R, Volkova O, Vasiliev A, Kataev V and Büchner B 2011 *Phys. Rev. B* **84** 134430.
- [32] Janson O, Tsirlin A A, Sichelschmidt J, Skourski Y, Weickert F and Rosner H 2011 *Phys. Rev. B* **83** 094435.
- [33] Belika A A, Azumaa M, Takanoa M 2004 *J. Solid State Chem.* **177** 883.
- [34] Belik A A, Uji S, Terashima T and Takayama-Muromachi E 2005 *J. Solid State. Chem.* **178** 3461.

FIGURES AND CAPTIONS

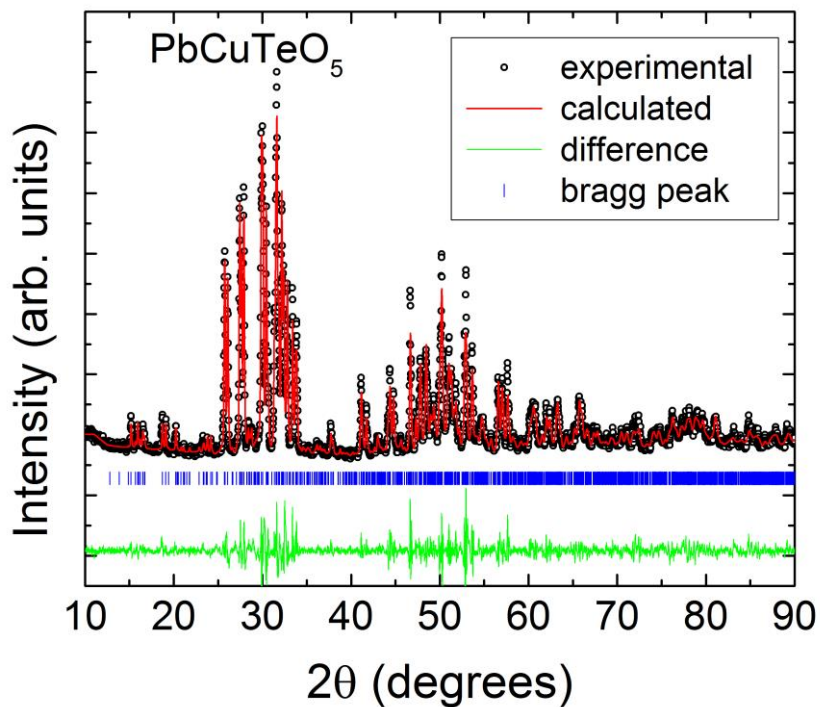


Figure 1: Powder XRD diffraction pattern for the polycrystalline samples of PbCuTeO_5 . The residual parameters obtained after Rietveld refinement are $R_p \approx 16.4\%$, $R_{wp} \approx 17.9\%$, $\underline{R}_{exp} \approx 6.80$, and $\chi^2 \approx 6.95$.

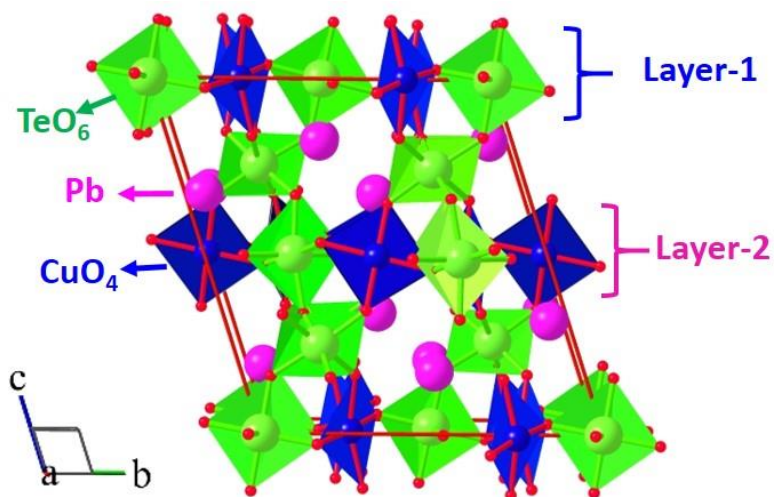
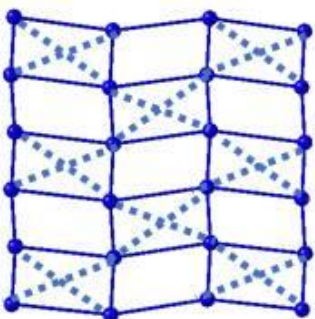
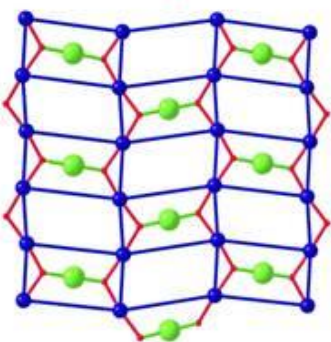
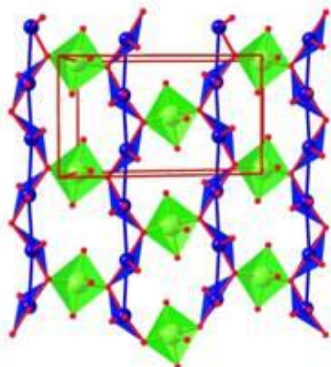


Figure 2: The triclinic unit cell of PbCuTeO_5 is built by Pb atoms, TeO_6 octahedral and CuO_4 squares. It comprises of two kinds of Cu layers; layer-1 ($z=0$) and layer-2 ($z=0.5$).

layer-1 with
dimer chains



Layer-2 with
trimer chains

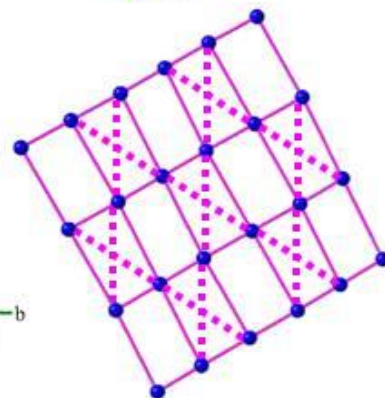
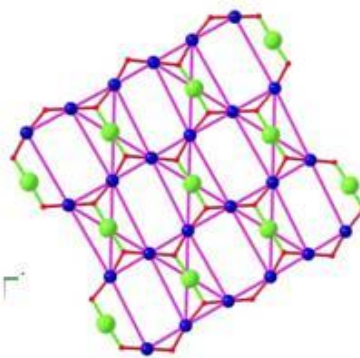
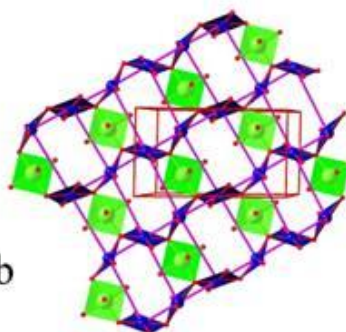


Figure 3: Two Cu layers (*ab*-planes) stacked alternatively. The first layer ($z=0$) consists of coupled dimer chains, while the second layer ($z=0.5$) with coupled trimer chains. The Cu-O-Cu chains are coupled each other via O-Te-O bonds forming the checkerboard lattice with anisotropic couplings.

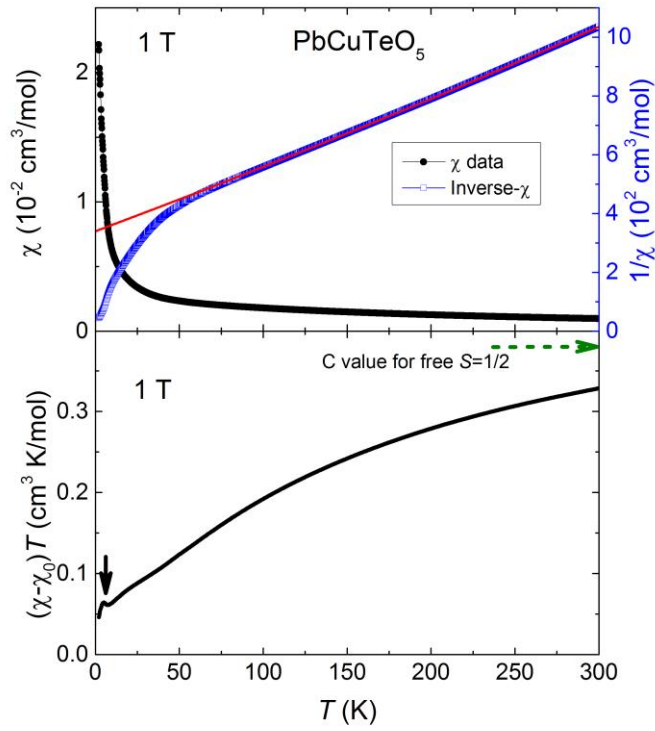


Figure 4: (a) The magnetic susceptibility $\chi(T)$ measured at 1 T and the $\chi^{-1}(T)$ data with a fit to Curie-Weiss law. (b) The plot of $(\chi - \chi_0)T$ versus T .

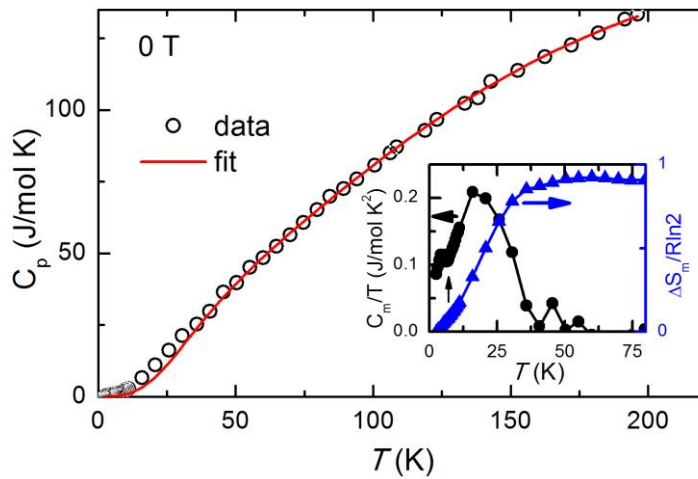


Figure 5: Specific heat (C_p) measured in zero-field. The red line indicates the fit to lattice contribution. Inset shows the magnetic specific heat divided by T i.e., C_m/T (left axis) and normalized magnetic entropy ($\Delta S_m/R \ln 2$) versus T (right axis).

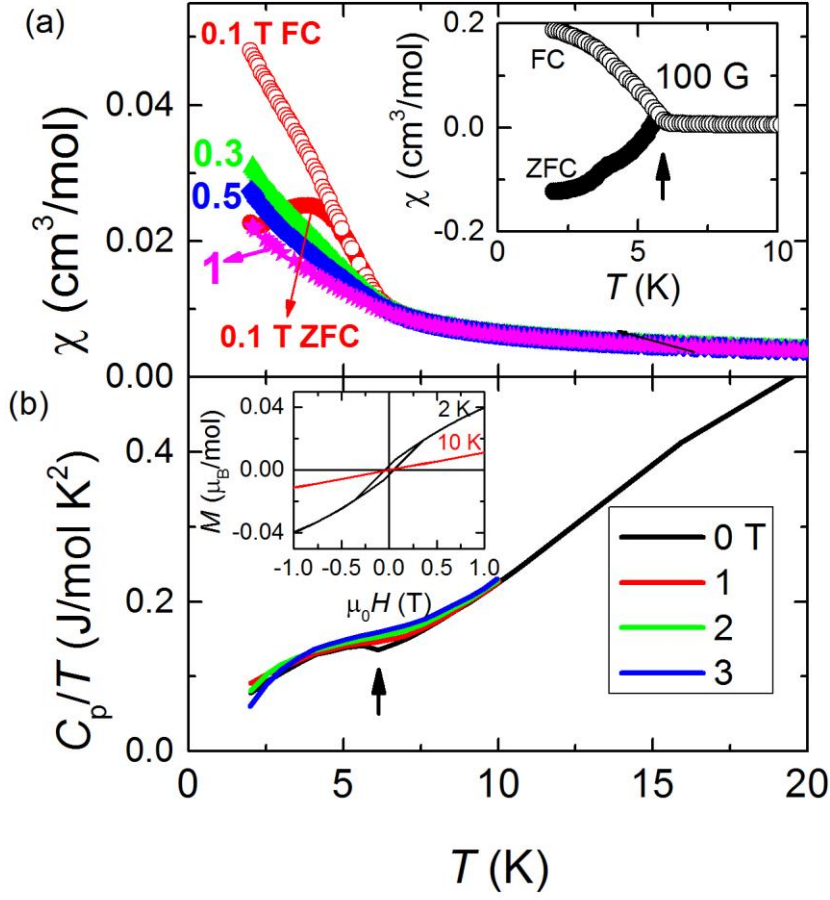


Figure 6: $\chi(T)$ at different fields. The inset shows the plot of ZFC and FC $\chi(T)$ at 100 G. (b) C_p/T versus T at different magnetic fields. Inset shows $M(H)$ data at 2 K and 10 K.

Table 1: The atomic coordinates and the occupancies obtained for PbCuTeO_5 after the Rietveld refinement at room temperature using the space group $P-1$ (No. 2).

Atoms	Wyckoff	x	y	z	Occupancy
Pb1	2i	0.986	0.562	0.176	1
Pb2	2i	0.490	0.448	0.329	1
Pb3	2i	0.014	0.944	0.323	1
Pb4	2i	0.513	0.0602	0.181	1

Cu1	2i	0.257	0.237	0.505	1
Cu2	2i	0.195	0.741	0.999	1
Cu3	1g	0	0.5000	0.5000	1
Cu4	2i	0.692	0.758	0.992	1
Cu5	1f	0.500	0	0.500	1
Te1	1a	0	0	0	1
Te2	2i	0.235	0.743	0.502	1
Te3	2i	0.467	0.764	0.248	1
Te4	1e	0.500	0.500	0	1
Te5	2i	0.948	0.745	0.747	1
O1	2i	0.981	0.650	0.461	1
O2	2i	0.445	0.651	0.962	1
O3	2i	0.481	0.844	0.533	1
O4	2i	0.019	0.919	0.840	1
O5	2i	0.618	0.834	0.156	1
O6	2i	0.392	0.602	0.5020	1
O7	2i	0.700	0.741	0.830	1
O8	2i	0.077	0.889	0.501	1
O9	2i	0.952	0.845	0.028	1
O10	2i	0.287	0.684	0.333	1
O11	2i	0.201	0.769	0.668	1
O12	2i	0.400	0.928	0.340	1
O13	2i	0.117	0.673	0.836	1
O14	2i	0.202	0.470	0.012	1
O15	2i	0.474	0.412	0.838	1
O16	2i	0.293	0.972	0.01	1
O17	2i	0.127	0.421	0.352	1
O18	2i	0.211	0.757	0.164	1
O19	2i	0.713	0.754	0.334	1
O20	2i	0.217	0.177	0.342	1

Table II: The bond angles and the bond lengths of the exchange couplings for PbCuTeO₅.

	Bond path	Bond length (Å)	Bond angle (°)
Layer-1 with dimer chains	Cu4-O9-Cu2	3.23	115.2
	Cu2-O2-Cu4	3.21	111.9
	Cu4-O9-Te1-O9-Cu2	5.68	Cu4-O9-Te1= 122.3 O9-Te1-O9= 180 Te1-O9-Cu2= 112
	Cu4-O9-Te1-O9-Cu4 (diagonal)	6.70	Cu4-O9-Te1= 122.3 O9-Te1-O9= 180 Te1-O9-Cu4= 112
Layer-2 with trimer chains	Cu1-O1-Cu3	3.43	Cu1-O1-Cu3=124.518
	Cu1-O3-Cu-5	3.10	Cu1-O3-Cu5=107.5
	Cu1-O1-Te2-O3-Cu1	5.62	Cu1-O1-Te2=110.4 O1-Te2-O3= 175.5 Te2-O3-Cu1= 117.5
	Cu1-O1-Te2-O3-Cu5 (diagonal)	6.49	Cu1-O1-Te2=110.4 O1-Te2-O3= 175.6 Te2-O3-Cu5= 112.3